Chapter 4
Using FRET to Determine How Myo10 Responds to Force in Filopodia

Francine Parker[1], Eulashini Chuntharpursat-Bon[2], Justin E. Molloy[3, 4] (iD),
and Michelle Peckham[1] (✉) (iD)

[1] Astbury Centre for Structural Molecular Biology & School of Molecular and Cellular Biology, Faculty of Biological Sciences, University of Leeds, Leeds, UK
f.parker@leeds.ac.uk; m.peckham@leeds.ac.uk
[2] Faculty of Medicine, University of Leeds, Leeds, UK
medechu@leeds.ac.uk
[3] The Francis Crick Institute, London, UK
[4] Centre for Mechanochemical Cell Biology, Warwick Medical School, Coventry, UK
justin.molloy@warwick.ac.uk

Abstract. Myosin 10 (Myo10) is an actin-based molecular motor that is essential for filopodia formation and likely senses tension through interactions with integrins in filopodial tips. It possesses a single α-helical (SAH) domain at the end of its canonical lever, which amplifies the movement of the motor. We have shown the SAH domain can contribute to lever function and possesses the properties of a constant force spring. Here we investigate whether the SAH domain plays a role in tension sensing and whether it becomes extended under load at the filopodial tip. Previously, we found that removing the entire SAH domain and short anti-parallel coiled coil (CC) region at the C-terminal end of the SAH does not prevent Myo10 from moving to filopodial tips in cells. Exploiting this, we generated recombinant forms of Myo10, in which a tension-sensing module (TSMod), comprising a FRET-pair YPet and mCherry separated by a linker sequence of amino acids was then inserted between the Myo10 motor and tail domains, so as to replace the SAH domain and CC region. The linker sequence comprised either a portion of the native SAH domain, or control sequences that were either short (x1: stiff) or long (x5: flexible) repeats of "GPGGA". As additional controls we also placed the TSMod construct at the N-terminus, where it should not experience force. Our FRET measurements indicate that the SAH domain of Myo10 may become extended at when the protein is stalled at the filopodial tips, so the SAH domain may therefore act as a force sensor.

Keywords: Myo10 · Myosin · Filopodia · FRET

Introduction

Filopodia are finger-like, membrane protrusions about 100 nm in diameter and up to several micrometres long that contain a bundle of 10–30 parallel actin filaments [1, 2]. They are dynamic cellular structures that interact with the environment, can adhere to the underlying substrate, and are also involved in phagocytosis. In mammalian cells, Myosin 10 (Myo10) is essential for filopodial formation [3]. Overexpression of Myo10 markedly increases the numbers of filopodia present on cells. Myo10 is an actin-based molecular motor that actively walks towards the distal, barbed ends, of the actin filament bundle and accumulates at the filopodial tip [4]. It comprises a motor domain, a lever with 3 IQ domains that bind calmodulin and calmodulin like protein [5] followed by a single α-helical domain (SAH) [6] that likely contributes to lever function [7] (Fig. 4.1a). The SAH is followed by a short stretch of residues (44) that can form an antiparallel coiled coil in vitro [8], a PEST domain, three pleckstrin homology (PH) domains that predominantly bind to PtdInsP3 [9, 10] followed by a myosin tail homology 4 (MyTH4) and a four point one ezrin moesin radixin (FERM) domain (Fig. 4.1a).

The tips of filopodia have many similarities to focal adhesions. A specific filopodial adhesion complex at the filopodial tips tethers filopodia to the underlying extracellular matrix and comprises many of the same proteins found in nascent focal adhesions, except for paxillin and focal adhesion kinase [11]. The continuous retrograde flow of actin from the filopodial tips, is similar to that observed for focal adhesions in the cell body [12]. In focal adhesions, the speed of retrograde flow is force dependent, reducing when force is high. Force is transmitted from the ECM to integrins, to proteins in the focal adhesions (e.g. talin) that interact with actin and in response, talin unfolds with the properties of a slip bond, whereas binding of integrins to the ECM shows the behaviour of a catch (or catch-slip) bond which holds tighter under increased load. In talin, three helical bundles unfold in three distinct steps and the first to unfold has been identified as the intial mechanosensing domain, unfolding at ~5 pN of force [13]. In filopodia, Myo10 could be involved in transmitting force from the ECM to the actin filament in filopodia. The FERM domain of Myo10 binds to the NPxY motif of β-integrins [14], and recently Myo10 was found to bind to and activate both α- and β-integrins at the filopodial tip increasing integrin binding affinity for extracellular matrix protein ligands [15]. Myo10 could therefore play a key role in mechanosensing in the filopodial tip. In this case, the SAH in Myo10 could be the force responsive element.

Nearly 20 years ago we discovered the SAH in Myo10 [6]. The amino acid sequence of the SAH domain is rich in E, R and K residues and we showed experimentally that it forms a stable alpha helix in aqueous solution. Its structural stability arises from multiple ionic interactions between E-K and E-R, 3 or 4 residues apart [6, 16, 17]. Critically, the SAH domain behaves as a constant force spring, rather than a Hookean spring as evidenced by its unfolding behaviour [18]. When the SAH domain is stretched, force at first rises by a small amount and then remains near-constant as the helix unfolds in a piece-wise manner. At filopodial tips, adhered to the surface, Myo10 could experience forces in the region of a few pN when it interacts with integrins, and this may cause the SAH domain to unfold. Its constant force behaviour would enable the motor to remain
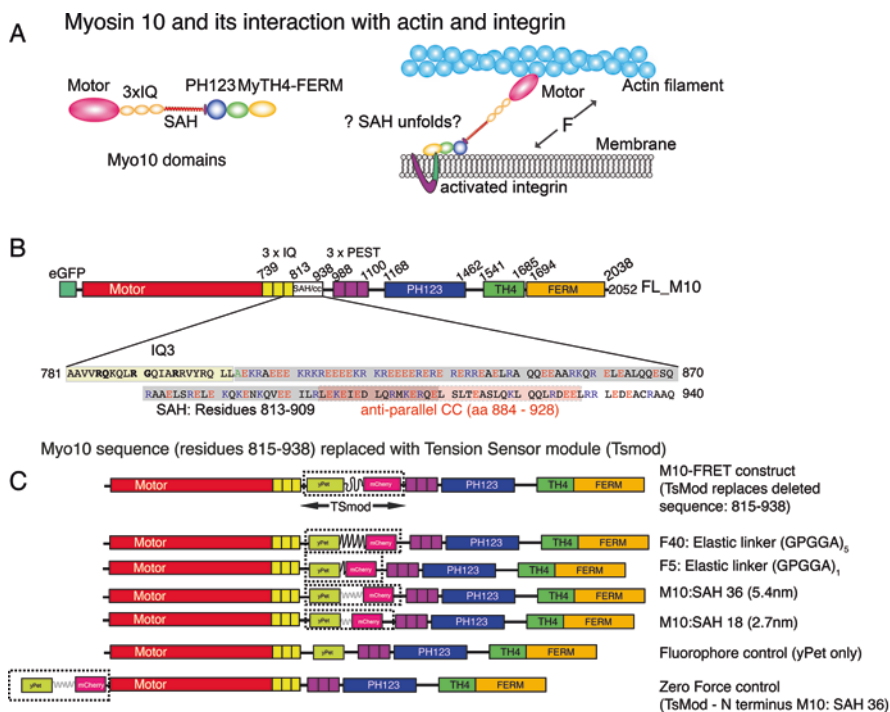
Fig. 4.1 Myo10 and FRET constructs. (**a**) The domains of Myo10 and its potential interaction between actin and integrins in filopodia. (**b**) A Myo10 construct in which residues 815–938 were deleted, deleting the SAH and anti-parallel CC, used to generate the FRET constructs used here. (**c**) Summary of the recombinant FRET constructs used in the current study.

attached to actin while the tail domains continue to bind integrins and/or other binding partners at the filopodial tip.

Here we have used an intramolecular FRET-based force sensor to determine if the SAH domain unfolds in situ at filopodial tips. A FRET-based force sensor was recently described for both vinculin and talin [19, 20] in which an elastic linker sandwiched between two fluorophores is inserted between two functional domains in the full-length protein. When force is low, these force sensors exhibit high FRET. When force (~1–6 pN) is applied to the protein *in vivo,* FRET decreases, and thus provides a read out of the response of the protein to load. We recently showed that removing the entire SAH domain (residues 814–938, M10-Δ3, bovine M10), including the anti-parallel coiled coil domain, does not prevent Myo10 from moving along actin bundles within the filopodia and accumulating at its tips, although its velocity drops to ~40% compared to the full-length, wild type protein [21]. We exploited this near-normal behaviour of the M10-ΔSAH construct by engineering in a FRET-based force sensor (replacing the entire SAH and anti-parallel coiled-coil domain) between the motor and the tail (Fig. 4.1b,c). Using this approach, we tested the unfolding behaviour of flagilliform elastic sequences, and two SAH sequences either 18 or 36 residues long from Myo10 using TIRFM and FLIM FRET approaches.

Methods

Constructs The full-length Myo10 construct (Bovine, P79114) with an N-terminal eGFP fusion (eGFP-M10) has been described previously ([4]). All Myo10 FRET sensors were adaptations of M10-Δ1, a full length bovine Myo10 construct with the SAH and CC region (residues 815–938) deleted [21] (Fig. 4.1b, c). To generate the FRET constructs, we inserted a tension sensor module (TS Mod) into M10-Δ1 to replace the deleted SAH and CC region (Fig. 4.1b, c). The TS Mods contained a 36 residue SAH domain (SAH36: the first 36 residues of Myo10 SAH), an 18 residue SAH domain (SAH18; the first 18 residues of Myo10 SAH), a short (F5: GPGGA) or a long flagelliform sequence (F40 GPGGAx5) sandwiched between the two fluorescent proteins, YPet and mCherry.

In addition, we generated single fluorophore controls, in which either yPet, or mCherry was inserted into the region of the deleted SAH and CC sequence in M10-Δ1 (Fig. 4.1c). The single fluorophore YPet control enabled us to measure the cross-talk (%) between green and red fluorescence channels on our imaging system and to measure the fluorescence life-time of YPet in zero-FRET conditions in FLIM-FRET experiments. As an additional control, we placed the SAH36 TSMod at the N-terminus of M10-Δ1. In this position, the TSMod is not expected to respond to force. All the constructs were synthesised by GenScript Biotech (The Netherlands). All constructs were cloned into pCDNA3.1 (+) expression plasmid and sequenced by GenScript. Maxipreps of the plasmid DNA were made according to the manufacturers' instructions (Qiagen).

Cell Culture HEK293 cells (ATCC, CRL-1573) or HeLa cells maintained in DMEM (Gibco, Life Technologies) supplemented with 10% FCS, 1% Penicillin-streptomycin, were seeded onto glass coverslips in 4-well plates 24 h before transfection with FuGene 6 (Promega), following the recommended protocol. After 24 h the cells were either fixed for 20 min in 2% PFA for staining or used for live-cell imaging.

Immunostaining Following fixation, the coverslips were washed x5 in PBS and permeabilised in 0.3% Triton-X for 5 minutes at RT, followed by blocking in 5% BSA in PBS-0.1% tween (PBS-T) for 1 hour and staining with DAPI and Alexa-546 phalloidin (Molecular Probes). A final wash step (x3 in PBS-T) was performed before coverslips were mounted in ProLong Gold Antifade mountant (Invitrogen) and cells were imaged using a Zeiss880 Airyscan or Deltavision deconvolution microscope.

Filopodia Analysis Deconvolution images were viewed in ImageJ and the number of filopodia per transfected cell were manually counted in a minimum of 15 cells from 3 replicate transfection experiments. Data was analysed using GraphPad Prism 9, and unpaired t-tests were used to compare differences between transfected cells.

TIRFM-FRET HeLa cells expressing myosin-10 FRET constructs were imaged using a two-camera TIRFM set-up using a wavelength of 488 nm to excite yPet (LaserHUB, Omicron, Germany). The FRET efficiency was measured in the acceptor (red or mCherry) channel, imaged using the filter FF01–589/40 nm (Semrock, USA). The bleed-though (cross-talk) signal was subtracted from the fluorescent signal using

yPet-myosin-10 data (9.8%). Bright Myo10 clusters at the filopodia tips were automatically detected using an automatic single particle tracking algorithm described previously [22]. FRET analysis was performed for these moving spots. Apparent FRET efficiency E_{app} was calculated as as $E_{app} = I_A/(I_A + I_D)$, where I_A and I_D represent acceptor and donor intensities, respectively [23].

FLIM-FRET Fluorescence life-time imaging was performed using a Leica SP8 confocal microscope for the Y-Pet only construct, the M10 18aa SAH TSMod, and the N-term TSMod constructs. The donor (yPet) fluorescence life-time was measured in the Myo10 clusters (bright spots) at the tips of filopodia and in the cell body, under zero-stress conditions. In order to calculate fluorescence lifetime, data were fitted to a single exponential decay and changes in FRET efficiency determined using *FLIMfit* [24].

Results

We generated a range of FRET constructs to test if the SAH domain could act as a force sensor by unfolding. In four of the constructs, a tension sensor module (TsMod) was inserted into the full length Myo10 construct, to replace the SAH domain and anti-parallel coiled coil (Fig. 4.1b,c). We designed four tension sensor modules (Fig. 4.1c), each of which contained the FRET pair: YPet and mCherry. As controls, we inserted sequences based on the flagelliform sequence (GPGGA) previously used for TsMod [20]. F40 (which has 5 repeats GPGGA repeats) allows forces between 1 and 6pN to be measured [20]. F5 has just one repeat, is expected to be stiffer than F40, and thus any reduction in the FRET signal resulting from strain will be smaller. To test the SAH domain unfolding behaviour, we inserted a long (36 residues: 5.4 nm in length) and a short (18 residues: 2.7 nm in length) region of SAH from Myo10. The 36 residue sequence was taken from the start of the SAH domain (KRAEEEKRKREEEEKRKREEEERERERERRREAELRA) and the 18 residue sequence comprised the first 18 residues of this sequence. As a further control, we placed the TsMod containing the 36 residue SAH domain at the N-terminus of Myo10 (Fig. 4.1c). The TsMod is not expected to experience force in this position, and thus we expect no change in FRET compared to TsMods inserted in the central region of the molecule.

Overexpression of Myo10 increases the number of filopodia and Myo10 localises to their tips [4], thus to confirm that the FRET constructs behaved as expected we first characterised filopodial number and location for each construct. We found that all the FRET constructs (Fig. 4.1c) correctly localised to the filopodial tips (Fig. 4.2a). This suggests that insertion of the TSMod did not adversely affect the ability of the Myo10 to localise to filopodial tips. Quantification of the numbers of filopodia in untransfected controls (cells not overexpressing Myo10 constructs) and for each of the constructs used in FRET experiments (Fig. 4.2b) showed that each of the constructs significantly increased the numbers of filopodia present, and by similar amounts, compared to untransfected cells. Therefore the Myo10 FRET constructs behave as expected.
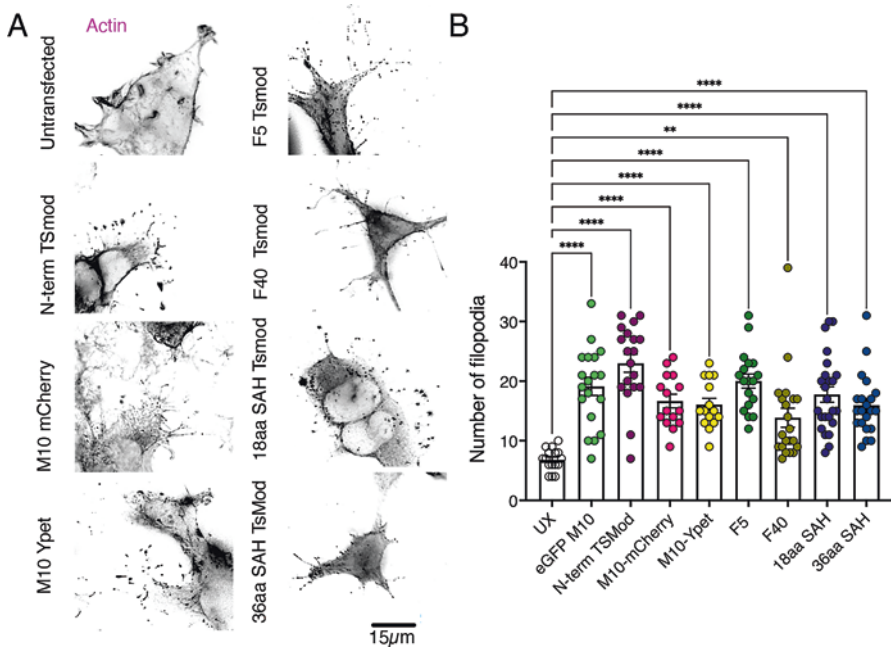
Fig. 4.2 Expression of Myo10 FRET constructs increases filopodial numbers. (**a**) Example images of untransfected cells (stained for actin) and each of the Myo10 constructs (except eGFP-M10) showing the staining for Myo10. Images from a minimum of 15 cells from 3 biological replicates, were characterised for number of filopodia (**b**). The mean numbers of filopodia per cell that result from the expression of each construct was compared to untransfected cells. Mean values ± S.E.M are shown. All of the constructs resulted in a significant increase in the numbers of filopodia per cell compared to untransfected (UX) cells. (****$p < 0.001$, **$P < 0.01$).

TIRFM FRET and FLIM FRET Experiments

FRET constructs were imaged in live cells using TIRFM-FRET and an acceptor photobleaching strategy (Fig. 4.3a). The FRET efficiency for the control TSMod construct placed at the N-terminus of Myo10 was highest. This is consistent with our expectation that the TSMod should not experience force in this position, and therefore FRET efficiency should be high. The four experimental TSMod constructs in M10Δ1, that replace the endogenous SAH domain and CC were then tested. Of these, F5 showed the highest FRET efficiency levels, consistent with the short length of the linker sequence (GPGGA) and the expectation that this construct should be stiff and FRET should be high. Its FRET efficiency was much higher than the F40 TSMod (5xGPGGA), which is expected to be less stiff and exhibit lower FRET efficiency. For the two SAH TSMod constructs, the 18aa SAH showed a higher FRET efficiency than the longer 36aa SAH. All of the experimental TSMod constructs showed a lower FRET efficiency than the control N-terminal TSMod. This may indicate that the experimental TSMod constructs are experiencing force that results in some unfolding of the sequence between YPet and mCherry.

To explore this further, we performed FLIM FRET on live cells with a subset of the constructs. We analysed the signal for the filopodial regions only. Example fluorescent images for YPet and mCherry (Fig. 4.3b) for live cells expressing FRET constructs, show that in filopodia tips, FRET is apparently lower for the test TSMod construct (18aa SAH in M10Δ1) compared to the N-terminal TSMod control. In addition, FRET in filopodial tips is apparently lower than in the cell body for the test TSMod construct. This suggests that the SAH domain is being stretched in the test construct in the filopodial tips, thereby reducing FRET.

The FLIM-FRET data was quantified by measuring the fluorescence lifetimes for individual tracked fluorescent spots in filopodia. The measured lifetime for the YPet only construct was consistent with that expected (2701 ps) (Fig. 4.3c). The measured lifetime for the test TSMod construct (18aa SAH in M10Δ1) was significantly lower (2471 ps) than that for YPet, and significantly higher than the control TSMod N-terminal construct (2301 ps) (Fig. 4.3c). This is consistent with a reduction in FRET for the 18aa SAH TSMod compared to the N-terminal TSMod control. Thus, both the TIRFM FRET measurements and the FLIM FRET measurements suggest that the TSMod placed between the motor and the tail, is responding to strain by some amount of unfolding, resulting in a reduction in FRET. The measured differences are small, as we only measure the average lifetime for a mixed population of molecules, in which extension of the 18aa SAH domain (and thus lifetime change) is variable, but they are in a similar range to that previously reported for TSMod constructs using the focal adhesion protein, talin [25].

Discussion

Here, we have tested tension-sensing modules (TSMod) in which specific sequences are inserted between Ypet and mCherry and inserted between the myosin head and tail in Myo10 Δ1, replacing the endogenous SAH and coiled-coil region. The expectation was that if Myo10 experiences force in the filopodial tips, that could arise from the interaction of the motor with actin, and the interaction of the tail with integrins, then we should observe a reduction in FRET for these constructs, compared to a control construct in which the TSMod is placed at the N-terminus of Myo10. The FRET data we have obtained is consistent with this idea and provides initial evidence that Myo10 could indeed have a role as a force sensor in filopodial tips, and that the SAH domain could unfold and act as the force sensor.

Our findings raise the possibility that SAH domains could act as force sensors in other myosins. Myosins 6, 7a and 10 in the human myosin superfamily all contain a SAH instead of a predicted coiled coil [26] and SAHs are additionally present in many different myosins across eukaryotes [27]. In myosins, the SAH is normally found just after the lever, and while we have demonstrated that it is stiff enough to contribute to lever function its stiffness is about ten-fold lower than that of the canonical lever, comprised of IQ motifs bound to calmodulin [7]. Myosin 7a is enriched in the retina and in the cochlea, and in the cochlea it localises to tip links in the stereocilia in inner hair cells in the cochlea, where the motor interacts with actin bundles in the central region and membrane proteins (reviewed in [28]). Myo7a is thought to tension the tip links, and
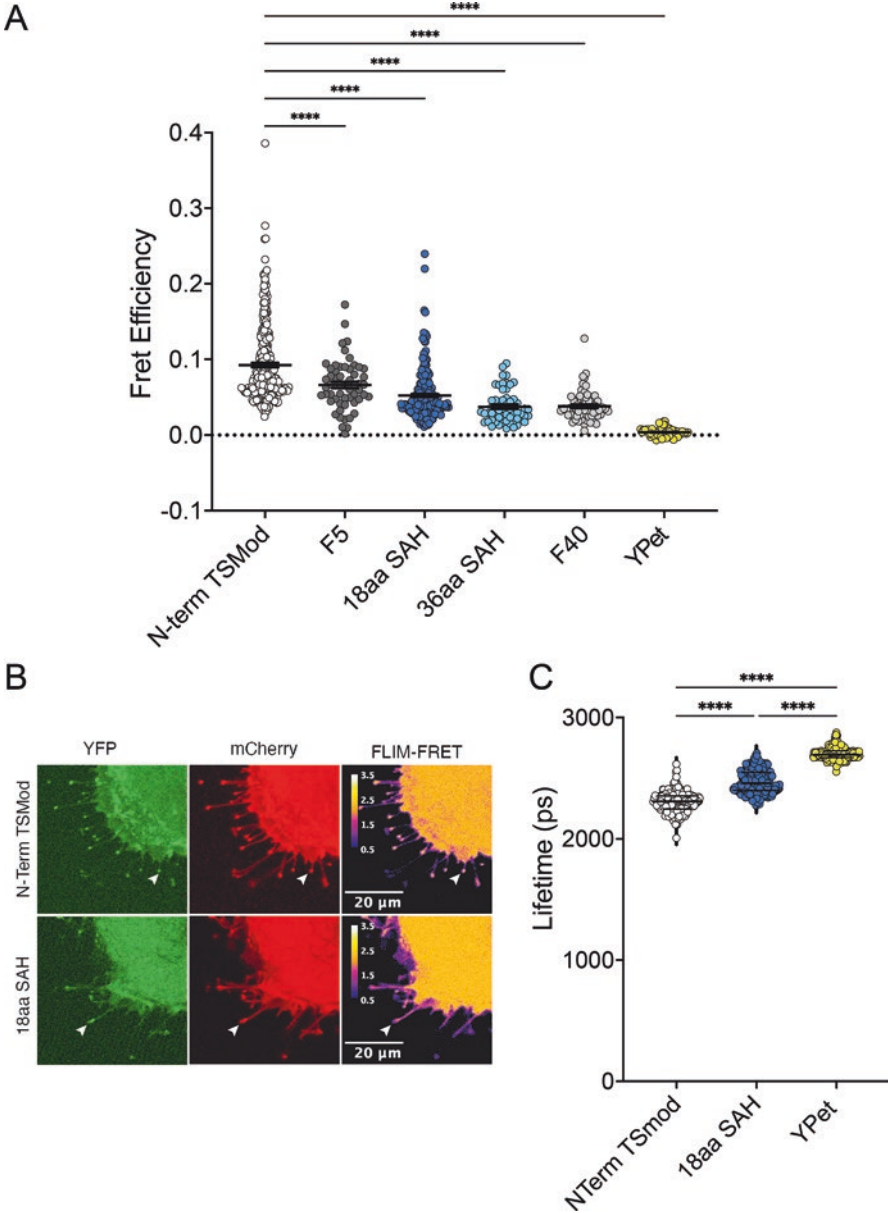
Fig. 4.3 TIRFM FRET and FLIM FRET measurements for TSMod constructs show reduced FRET. (**a**) TIRFM FRET measurements for individual fluorescent spots in the filopodium using live cells. N-Term TSMod is the 36 residue SAH control construct fused to the N-terminus of Myo10. F5, 18aa SAH 36aa SAH and F40 are the 4 TSMod constructs inserted in Myo10Δ1 (Fig. 4.1c). YPet is a control construct in which YPet is inserted into Myo10 as described (Fig. 4.1c). Data are shown as scatter dot plot with mean ± S.E.M. Values for each of the TSMod constructs and YPet were compared to the N-terminal TSMod control. (**b**) Shows averaged

thus force sensitivity in Myo7a could be important for this function. Myo6 is widely expressed and it is less clear how it would employ a force sensing function, unless this becomes important in its role as an organelle anchor [29].

It would be interesting to explore if SAHs present in a range of other proteins [26] could also contribute to a strain-dependent function. For example, we previously suggested that the long (32 nm) SAH in the protein inner centromere protein, INCENP, could potentially stretch up to 80 nm [30] acting as a flexible dog-leash. The question now would be if this is purely a passive function of the SAH, or whether it is somehow responding to strain. Finally, while these initial tests appear to demonstrate that the SAH domain could unfold in response to force or strain, it would be interesting to determine how this might be modulated, for example by the type of extracellular substrate, or if it is affected by retrograde flow of actin, as found for talin and vinculin in focal adhesions.

References

1. Svitkina TM, Bulanova EA, Chaga OY, Vignjevic DM, Kojima S, Vasiliev JM et al (2003) Mechanism of filopodia initiation by reorganization of a dendritic network. J Cell Biol 160(3):409–421. https://doi.org/10.1083/jcb.200210174
2. Small JV, Celis JE (1978) Filament arrangements in negatively stained cultured cells: the organization of actin. Cytobiologie 16(2):308–325
3. Berg JS, Derfler BH, Pennisi CM, Corey DP, Cheney RE (2000) Myosin-X, a novel myosin with pleckstrin homology domains, associates with regions of dynamic actin. J Cell Sci 113(Pt 19):3439–3451
4. Berg JS, Cheney RE (2002) Myosin-X is an unconventional myosin that undergoes intrafilopodial motility. Nat Cell Biol 4(3):246–250. https://doi.org/10.1038/ncb762
5. Bennett RD, Strehler EE (2008) Calmodulin-like protein enhances myosin-10 translation. Biochem Biophys Res Commun 369(2):654–659. https://doi.org/10.1016/j.bbrc.2008.02.056

Fig. 4.3 (continued) (10 frames, 0.75 frames per second) fluorescent images for YFP and mCherry for the N-terminal TSMod construct (control) and the 18aa SAH TSMod construct inserted into Myo10 Δ1 together with the associated FLIM-FRET lifetime map from live cells. Arrows indicate one of the many filopodia. Note that because the difference in lifetime is relatively small it is difficult to see on the psuedocolor lifetime maps (right panels). (**c**) Shows the fluorescence lifetime data from FLIM-FRET experiments, in which a single lifetime was fitted to the data. Measurements were made by tracking individual spots within single filopodia for a minimum of 3 cells. Statistical comparisons as shown. **** is equivalent to $p < 0.0001$.

6. Knight PJ, Thirumurugan K, Xu Y, Wang F, Kalverda AP, Stafford WF 3rd et al (2005) The predicted coiled-coil domain of myosin 10 forms a novel elongated domain that lengthens the head. J Biol Chem 280(41):34702–34708. https://doi.org/10.1074/jbc.M504887200

7. Baboolal TG, Sakamoto T, Forgacs E, White HD, Jackson SM, Takagi Y et al (2009) The SAH domain extends the functional length of the myosin lever. Proc Natl Acad Sci U S A 106(52):22193–22198. https://doi.org/10.1073/pnas.0909851106

8. Lu Q, Ye F, Wei Z, Wen Z, Zhang M (2012) Antiparallel coiled-coil-mediated dimerization of myosin X. Proc Natl Acad Sci U S A 109(43):17388–17393. https://doi.org/10.1073/pnas.1208642109

9. Isakoff SJ, Cardozo T, Andreev J, Li Z, Ferguson KM, Abagyan R et al (1998) Identification and analysis of PH domain-containing targets of phosphatidylinositol 3-kinase using a novel in vivo assay in yeast. EMBO J 17(18):5374–5387. https://doi.org/10.1093/emboj/17.18.5374

10. Umeki N, Jung HS, Sakai T, Sato O, Ikebe R, Ikebe M (2011) Phospholipid-dependent regulation of the motor activity of myosin X. Nat Struct Mol Biol 18(7):783–788. https://doi.org/10.1038/nsmb.2065

11. Jacquemet G, Stubb A, Saup R, Miihkinen M, Kremneva E, Hamidi H et al (2019) Filopodome mapping identifies p130Cas as a mechanosensitive regulator of filopodia stability. Curr Biol 29(2):202–16 e7. https://doi.org/10.1016/j.cub.2018.11.053

12. Bornschlogl T, Romero S, Vestergaard CL, Joanny JF, Van Nhieu GT, Bassereau P (2013) Filopodial retraction force is generated by cortical actin dynamics and controlled by reversible tethering at the tip. Proc Natl Acad Sci U S A 110(47):18928–18933. https://doi.org/10.1073/pnas.1316572110

13. Yao M, Goult BT, Chen H, Cong P, Sheetz MP, Yan J (2014) Mechanical activation of vinculin binding to talin locks talin in an unfolded conformation. Sci Rep 4:4610. https://doi.org/10.1038/srep04610

14. Zhang H, Berg JS, Li Z, Wang Y, Lang P, Sousa AD et al (2004) Myosin-X provides a motor-based link between integrins and the cytoskeleton. Nat Cell Biol 6(6):523–531. https://doi.org/10.1038/ncb1136

15. Miihkinen M, Gronloh MLB, Popovic A, Vihinen H, Jokitalo E, Goult BT et al (2021) Myosin-X and talin modulate integrin activity at filopodia tips. Cell Rep 36(11):109716. https://doi.org/10.1016/j.celrep.2021.109716

16. Wolny M, Batchelor M, Bartlett GJ, Baker EG, Kurzawa M, Knight PJ et al (2017) Characterization of long and stable de novo single alpha-helix domains provides novel insight into their stability. Sci Rep 7:44341. https://doi.org/10.1038/srep44341

17. Batchelor M, Wolny M, Baker EG, Paci E, Kalverda AP, Peckham M (2019) Dynamic ion pair behavior stabilizes single alpha-helices in proteins. J Biol Chem 294(9):3219–3234. https://doi.org/10.1074/jbc.RA118.006752

18. Wolny M, Batchelor M, Knight PJ, Paci E, Dougan L, Peckham M (2014) Stable single alpha-helices are constant force springs in proteins. J Biol Chem 289(40):27825–27835. https://doi.org/10.1074/jbc.M114.585679

19. Ringer P, Weissl A, Cost AL, Freikamp A, Sabass B, Mehlich A et al (2017) Multiplexing molecular tension sensors reveals piconewton force gradient across talin-1. Nat Methods 14(11):1090–1096. https://doi.org/10.1038/nmeth.4431

20. Grashoff C, Hoffman BD, Brenner MD, Zhou R, Parsons M, Yang MT et al (2010) Measuring mechanical tension across vinculin reveals regulation of focal adhesion dynamics. Nature 466(7303):263–266. https://doi.org/10.1038/nature09198

21. Baboolal TG, Mashanov GI, Nenasheva TA, Peckham M, Molloy JE (2016) A combination of diffusion and active translocation localizes myosin 10 to the filopodial tip. J Biol Chem 291(43):22373–22385. https://doi.org/10.1074/jbc.M116.730689

22. Mashanov GI, Molloy JE (2007) Automatic detection of single fluorophores in live cells. Biophys J 92(6):2199–2211. https://doi.org/10.1529/biophysj.106.081117
23. Roy R, Hohng S, Ha T (2008) A practical guide to single-molecule FRET. Nat Methods 5(6):507–516. https://doi.org/10.1038/nmeth.1208
24. Warren SC, Margineanu A, Alibhai D, Kelly DJ, Talbot C, Alexandrov Y et al (2013) Rapid global fitting of large fluorescence lifetime imaging microscopy datasets. PLoS One 8(8):e70687. https://doi.org/10.1371/journal.pone.0070687
25. Austen K, Ringer P, Mehlich A, Chrostek-Grashoff A, Kluger C, Klingner C et al (2015) Extracellular rigidity sensing by talin isoform-specific mechanical linkages. Nat Cell Biol 17(12):1597–1606. https://doi.org/10.1038/ncb3268
26. Peckham M, Knight PJ (2009) When a predicted coiled coil is really a single alpha-helix, in myosins and other proteins. Soft Matter 5(13):2493–2503. https://doi.org/10.1039/b822339d
27. Simm D, Hatje K, Kollmar M (2017) Distribution and evolution of stable single alpha-helices (SAH domains) in myosin motor proteins. PLoS One 12(4):e0174639. https://doi.org/10.1371/journal.pone.0174639
28. Moreland ZG, Bird JE (2022) Myosin motors in sensory hair bundle assembly. Curr Opin Cell Biol 79:102132. https://doi.org/10.1016/j.ceb.2022.102132
29. Zakrzewski P, Lenartowska M, Buss F (2021) Diverse functions of myosin VI in spermio-genesis. Histochem Cell Biol 155(3):323–340. https://doi.org/10.1007/s00418-020-01954-x
30. Samejima K, Platani M, Wolny M, Ogawa H, Vargiu G, Knight PJ et al (2015) The inner centromere protein (INCENP) coil is a single alpha-helix (SAH) domain that binds directly to microtubules and is important for chromosome passenger complex (CPC) localization and function in mitosis. J Biol Chem 290(35):21460–21472. https://doi.org/10.1074/jbc.M115.645317